Probing the Active Site of Cytochrome P450 2B1: Metabolism of 7-Alkoxycoumarins by the Wild Type and Five Site-Directed Mutants†

Yasuna Kobayashi,‡,§ Xiaojun Fang,§,|| Grazyna D. Szklarz, and James R. Halpert*

Department of Pharmacology and Toxicology, College of Pharmacy, The University of Arizona, Tucson, Arizona 85721

Received December 23, 1997; Revised Manuscript Received March 16, 1998

ABSTRACT: A series of 7-alkoxycoumarins (chain length of 1−7 carbon atoms) was utilized as active site probes of purified *Escherichia coli*-expressed cytochrome P450 2B1 wild type and five site-directed mutants (I114V, F206L, V363A, V363L, and G478S). The production of 7-hydroxycoumarin, the O-dealkylation product, by the wild-type enzyme exhibited a rank order of C2 > C4 > C3 > C1 > C5 > C6 = C7. The pattern observed for the P450 I114V mutant was similar to that of the wild-type enzyme, whereas with F206L and G478S mutants, the rate of O-dealkylation was low with all the compounds. In contrast, with V363A, the highest rate of product formation was observed with 7-butoxycoumarin. The V363L mutant preferentially catalyzed the O-dealkylation of 7-methoxy- and 7-ethoxycoumarin, and a further increase in the length of the alkyl chain led to a marked decrease in product formation. The stoichiometry of 7-butoxycoumarin oxidation by V363L suggested that products other than 7-hydroxycoumarin were also formed. HPLC and GC−EIMS analyses revealed that P450 2B1 V363L produced 7-(3-hydroxybutoxy)-coumarin and 7-(4-hydroxybutoxy)coumarin as major oxidation products, while the V363A mutant mainly catalyzed the O-dealkylation of 7-butoxycoumarin. Docking of alkoxycoumarins into the active site of a P450 2B1 homology model confirmed the importance of the studied residues in substrate dealkylation and explained the formation of novel 7-butoxycoumarin products by the V363L mutant.

The cytochrome P450 superfamily plays an important role in the detoxification and metabolic activation of a large number of endogenous and exogenous compounds, such as drugs, carcinogens, and environmental chemicals. Any given P450[1] enzyme can usually metabolize a number of different substrates, and individual isoforms often exhibit discrete but overlapping substrate specificities (*1*−*3*). An intriguing question is the molecular basis of the unique specificity of each enzyme. Cytochromes P450 of the 2B subfamily are known to oxidize a wide range of drugs and chemicals in the liver of rats (*4*−*9*), rabbits **(***10*, *11*), and dogs (*12*−*14*) and have provided an excellent model system for structure−function analysis. Recent studies in our laboratory utilizing site-directed mutagenesis have revealed that residues 114, 206, 209, 290, 294, 302, 363, 367, 477, 478, and 480 determine the substrate specificity and regio- and stereoselectivity of P450 2B enzymes (*4*−*8*, *10*−*18*). All of these residues are located within substrate recognition sites (SRSs) of P450 2B1 and have counterparts in active site residues of mammalian P450 2A and 2C subfamilies (reviewed in ref *19*) and in bacterial P450s such as P450 101 and 102 (*20*, *21*).

Studies of P450 101 and mutants have recently revealed interesting correlations between the identity and location of key residues and the efficiency of coupling of pyridine nucleotide-derived reducing equivalents to product formation (*20*, *21*). With the preferred substrate camphor, P450 101 yields 1 mol of product for each mole of NADPH consumed (*22*, *23*), whereas uncoupling is observed during the metabolism of other substrates such as ethylbenzene (*20*). Recently, we investigated the stoichiometry of 7-ethoxycoumarin metabolism by the P450 2B1 wild type and mutants and found that the efficiency of coupling of reducing equivalents to 7-hydroxycoumarin formation was decreased for all mutants studied except I114V (*24*). Uncoupling to H_2O was increased for F206L, V363A, and G478S, decreased for V363L, and unchanged for I114V. Uncoupling to H_2O_2 was increased for V363L and decreased for I114V, F206L, and V363A. These findings provided biochemical support for the concept that residues 206, 363, and 478 comprise part of the substrate binding site of P450 2B1.

7-Alkoxycoumarins, such as 7-methoxy-, 7-ethoxy-, and 7-propoxycoumarins, are metabolized by P450 2B enzymes in the liver of phenobarbital-treated experimental animals (*9*, *25*−*31*). Okuno et al. (*25*) and Matsubara et al. (*31*) have suggested that the differences in 7-alkoxycoumarin

† Supported by Grant ES03619 and Center Grant ES06694 from the National Institutes of Health.

* To whom correspondence and reprint requests should be addressed. Phone: (520) 626-4358. Fax: (520) 626-2466. E-mail: Halpert@pharmacy.arizona.edu.

‡ Present address: Department of Clinical Pharmacy, School of Pharmaceutical Sciences, Showa University, 1-5-8 Hatanodai, Shinagawa-Ku, Tokyo 142, Japan.

§ Y.K. and X.F. contributed equally to this work.

|| Present address: Department of Drug Metabolism, Merck Research Laboratories, West Point, PA 19486.

[1] Abbreviations: P450, cytochrome P450; CHAPS, 3-[(3-cholamidopropyl)dimethylammonio]-1-propanesulfonic acid; EDTA, ethylenediaminetetraacetic acid; HEPES, 4-(2-hydroxyethyl)-1-piperazineethanesulfonic acid; DLPC, dilauroyl-L-3-phosphatidylcholine; HPLC, high-performance liquid chromatography; SDS−PAGE, sodium dodecyl sulfate−polyacrylamide gel electrophoresis; TLC, thin-layer chromatography; DMSO, dimethyl sulfoxide; GC−EIMS, gas chromatography−electron impact mass spectrometry.

S0006-2960(97)03145-0 CCC: $15.00
Published on Web 04/22/1998

O-dealkylase activities of liver microsomes from experimental animals reflect the variation in P450 isoforms present. Thus, the O-dealkylation of 7-alkoxycoumarins has been utilized to determine metabolic differences between P450 isoforms using xenobiotic-induced microsomes from liver, kidney, intestine, lung, and cultured hepatocytes (*9*, *25*−*28*). All of these findings suggest that 7-alkoxycoumarins would be good probes for investigating the role of key residues in P450 2B1. Except for 7-ethoxycoumarin (*24*), there are no data dealing with 7-alkoxycoumarins as active site probes of P450 2B1 and mutants.

In this study, we examined the effect of chain length on the metabolism of 7-substituted alkoxycoumarins (1−7 carbon atoms) by the *Escherichia coli*-expressed purified P450 2B1 wild type and five site-directed mutants (I114V, F206L, V363A, V363L, and G478S). Furthermore, we investigated the stoichiometry of 7-butoxycoumarin oxidation by recombinant P450 2B1 V363A and V363L and determined the structures of metabolites produced. The experimental results were successfully interpreted using molecular modeling.

EXPERIMENTAL PROCEDURES

Materials. The pKK233-2 *E. coli* expression plasmid was purchased from Pharmacia (Alameda, CA), and Topp3 cells were from Stratagene (La Jolla, CA). Growth media for *E. coli* were obtained from Difco (Detroit, MI). Recombinant NADPH−cytochrome P450 reductase and cytochrome b_5 were obtained as described (*32*). 7-(Benzyloxy)resorufin, 7-(pentyloxy)resorufin, resorufin, NADPH, dimethyl sulfoxide, and CHAPS were purchased from Sigma Chemical Co. (St. Louis, MO). HEPES was obtained from CalBiochem Corp. (La Jolla, CA). Thin-layer chromatography plates [silica gel, 250 μM, Si 250 F (C19)] were purchased from J. T. Baker, Inc. (Phillipsburg, NJ). 7-Alkoxycoumarins were synthesized by E. Mash (Department of Chemistry, The University of Arizona). All other chemicals used were of the highest grade available and were obtained from standard commercial sources.

Synthesis of Butoxycoumarin Metabolite Standards. 7-(3-Butenyloxy)coumarin. To a suspension of NaH (334 mg, 13.88 mmol) in 40 mL of freshly distilled THF and 40 mL of DMSO at 25 °C was added 7-hydroxycoumarin (1.5 g, 9.25 mmol) in one portion. After the mixture was stirred for 10 min, 4-bromo-1-butene was added in one portion and the mixture was heated to reflux for 3 h. The solution was cooled to room temperature and poured into 100 mL of 0.5 N HCl and diluted with water to dissolve the remaining solids. The water layer was extracted with 3 × 130 mL of diethyl ether, and then the organic layers were combined, dried over $MgSO_4$, filtered, and concentrated in vacuo. The resulting yellowish oil was purified on 200 mL of 230/400 silica with 12% ethyl acetate/hexanes to yield 921 mg (4.26 mmol, 46%) of a yellowish solid (R_f = 0.40, 40% ethyl acetate/hexanes) that was recrystallized from 2% ethyl acetate/pentanes to yield colorless needles (mp 49−50 °C). IR (NaCl, neat): 1047, 1132, 1234, 1294, 1362, 1421, 1506, 1574, 1609, 1736 cm^{-1}. ^{1}H NMR (199.975 MHz, $CDCl_3$): δ 2.53−2.63 (2H, m), 4.08 (2H, t, J = 6.7 Hz), 5.11−5.25 (2H, m), 5.91 (1H, ddt, J = 17.1 Hz, J = 10.3 Hz, J = 6.7 Hz), 6.25 (1H, d, J = 9.5 Hz), 6.80−6.87 (2H, m), 7.37 (1H, d, J = 8.3 Hz), 7.64 (1H, d, J = 9.5 Hz). ^{13}C NMR (50.289 MHz, $CDCl_3$): δ 33.3 (CH_2), 67.7 (CH_2), 101.3 (CH), 112.5 (C), 112.9 (CH), 113.0 (CH), 117.5 (CH_2), 128.7 (CH), 133.8 (CH), 143.4 (CH), 155.8 (C), 161.2 (C), 162.1 (C).

7-(3-Hydroxybutoxy)coumarin. Mercuric acetate (146 mg, 0.46 mmol) was dissolved in 1 mL of H_2O, and then 1 mL of freshly distilled THF and 7-(3-butenyloxy)coumarin (100 mg, 0.46 mmol) were added in succession. The mixture was stirred until a clear and colorless solution resulted, and then 1 mL of a 3 N solution of NaOH was added followed by a solution of $NaBH_4$ (18.9 mg, 0.50 mmol) in 1 mL of 3 N NaOH. This was stirred slowly for 30 min to allow the metallic mercury to coagulate. The water layer was then saturated with NaCl and extracted with 4 × 10 mL of diethyl ether. The organic layers were combined, dried over $MgSO_4$, filtered, and removed in vacuo to give a clear, colorless oil. This was purified on 100 mL of 230/400 silica with 50% ethyl acetate/hexanes to yield 57 mg (0.24 mmol, 53%) of a cloudy colorless oil (R_f = 0.08, 40% ethyl acetate/hexanes) that crystallized (mp 50−52 °C) upon standing at room temperature. IR (NaCl, neat): 919, 1129, 1227, 1345, 1400, 1511, 1555, 1616, 1740, 3444 cm^{-1}. ^{1}H NMR (199.975 MHz, $CDCl_3$): δ 1.30 (3H, d, J = 6.3 Hz), 1.88−2.01 (2H, m), 2.28 (1H, br s), 4.07−4.28 (3H, m), 6.23 (1H, d, J = 9.4 Hz), 6.79−6.87 (2H, m), 7.36 (1H, d, J = 8.4 Hz), 7.63 (1H, d, J = 9.5 Hz). ^{13}C NMR (50.289 MHz, $CDCl_3$): δ 23.8 (CH_3), 37.9 (CH_2), 65.2 (CH), 65.9 (CH_2), 101.3 (CH), 112.4 (C), 112.8 (CH), 112.9 (CH), 128.7 (CH), 143.4 (CH), 155.7 (C), 161.3 (C), 162.0 (C).

7-[4-(tert-Butyldimethylsiloxy)butoxy]coumarin. To a well-stirred mixture of 7-hydroxycoumarin (1.11 g, 6.8 mmol) and NaH (0.17 g, 7.1 mmol) in methyl sulfoxide (10 mL, distilled from calcium hydride) under argon was added 4-(*tert*-butyldimethylsiloxy)butyl iodide (1.63 g, 5.20 mmol). The mixture was allowed to stir at 70 °C for 24 h. After the solution cooled to room temperature, 10% NaOH (50 mL) was added. The mixture was extracted with diethyl ether (3 × 75 mL). The ether extracts were combined, dried ($MgSO_4$), filtered, and concentrated in vacuo to a yellow oil on a rotary evaporator. This was chromatographed on silica gel 60 (30 g, 230−400 mesh) using 20% ethyl acetate/hexanes to provide 7-[4-(*tert*-butyldimethylsiloxy)butoxy]-coumarin (0.46 g, 1.3 mmol, 25%) (R_f = 0.59, 50% ethyl acetate/hexanes) as a pale yellow solid (mp 60−61 °C). IR (Nujol): 3082 (weak), 3052 (weak), 1724, 1612, 1463, 1128, 99.3, 830, 773 cm^{-1}. ^{1}H NMR (300 MHz, $CDCl_3$): δ 0.03 (6H, s), 0.87 (9H, s), 1.67 (2H, tt, J = 6.1 Hz, J = 6.6 Hz), 1.87 (2H, tt, J = 6.3 Hz, J = 6.6 Hz), 3.66 (2H, t, J = 6.1 Hz), 4.02 (2H, t, J = 6.3 Hz), 6.21 (1H, d, J = 9.4 Hz), 6.77 (1H, d, J = 2.1 Hz), 6.80 (1H, dd, J = 2.1 Hz, J = 8.3 Hz), 7.33 (1H, d, J = 8.3 Hz), 7.61 (1H, d, J = 9.4 Hz). ^{13}C NMR (75 MHz, $CDCl_3$): δ 5.3, 18.3, 25.6, 25.9, 29.1, 62.6, 68.4, 101.3, 112.3, 112.9, 112.9, 128.7, 143.4, 155.9, 161.2, 162.3. Mass spectrum [70 eV, *m*/*z* (relative intensity)]: 348 (0.01), 292 (3.6), 291 (16.8), 250 (11.2), 249 (65.7), 220 (16.2), 219 (100), 163 (23.1).

7-(4-Hydroxybutoxy)coumarin. A mixture of 7-[4-(*tert*-butyldimethylsiloxy)butoxy]coumarin (0.45 g, 1.3 mmol) and tetrabutylammonium fluoride (1 M in THF, 2.0 mL, 2.0 mmol) was allowed to stir at room temperature for 0.5 h.

Then, HCl (12 M, 0.2 mL, 2.4 mmol) was added. After 2 h at room temperature, the reaction mixture was loaded onto a column containing silica gel 60 (30 g, 230−400 mesh) and eluted with 50% ethyl acetate/hexanes to provide 7-(4-hydroxybutoxy)coumarin (0.25 g, 1.1 mmol, 85%) (R_f = 0.13, 50% ethyl acetate/hexanes) as a white solid (mp 74−76 °C). IR (Nujol): 3418 (broad), 1699, 1613, 1465, 1354, 1131, 1049, 838 cm^{-1}. ^1H NMR (300 MHz, $CDCl_3$): δ 1.66 (2H, tt, J = 6.2 Hz, J = 6.5 Hz), 1.84 (2H, tt, J = 6.2 Hz, J = 6.5 Hz), 2.70 (1H, s), 3.65 (2H, t, J = 6.2 Hz), 3.96 (2H, t, J = 6.2 Hz), 6.13 (1H, d, J = 9.3 Hz), 6.67 (1H, d, J = 2.2 Hz), 6.73 (1H, dd, J = 2.2 Hz, J = 8.5 Hz), 7.27 (1H, d, J = 8.5 Hz), 7.56 (1H, d, J = 9.3 Hz). ^{13}C NMR (75 MHz, $CDCl_3$): δ 25.3, 28.9, 61.9, 68.2, 101.1, 112.2, 112.5, 112.7, 128.6, 143.5, 155.5, 161.3, 162.0. Mass spectrum [70 eV, *m*/*z* (relative intensity)]: 235 (0.6), 234 (3.0), 164 (1.8), 163 (17.8), 162 (62.4), 134 (100).

Purification of E. coli-Expressed P450 2B1 and Mutants. The P450 2B1 wild type and I114V, F206L, V363A, V363L, and G478S mutants were expressed in an *E. coli* system as described (*8*), and the enzymes were purified using a two-column protocol (*33*) with some modifications. All purification procedures were performed at 4 °C. A CHAPS-solubilized membrane preparation representing 50−100 nmol of P450 (L of culture)$^{-1}$ with a specific content of >1 nmol (mg of protein) $^{-1}$ was diluted with 1 bed volume of buffer A [100 mM potassium phosphate, 20% glycerol, and 1.0 mM EDTA (pH 7.5)] and applied [5−6 nmol of P450 (mL of gel)$^{-1}$] onto an *n*-octylamino-Sepharose (OAS) column (14 × 85 mm) that had been pre-equilibrated with 4 bed volumes of buffer B [100 mM potassium phosphate, 20% glycerol, 1 mM EDTA, and 0.6% sodium cholate (pH 7.5)]. Subsequently, the OAS column was washed with 10 bed volumes of buffer C [100 mM potassium phosphate, 20% glycerol, 1 mM EDTA, and 0.5% sodium cholate (pH 7.5)] at a flow rate of 20 mL h^{-1}. P450 proteins were then eluted with buffer D [100 mM potassium phosphate, 20% glycerol, 1 mM EDTA, 0.4% sodium cholate, and 0.1% Emulgen 913 (pH 7.5)] at a flow rate of 9 mL h^{-1}. Cytochrome P450 was detected spectrophotometrically at 417 nm, and the fractions containing the enzyme were pooled and dialyzed overnight against 2 L of buffer E [10 mM potassium phosphate and 20% glycerol (pH 6.5)]. Removal of the detergent was achieved on a 5 mL hydroxyapatite column (HA, 14 × 85 mm) pre-equilibrated with 4 bed volumes of buffer E. After application of the dialyzed P450 preparation, the HA column was washed with 10 bed volumes of buffer E at a flow rate of 20 mL h^{-1}. The P450 protein was eluted from the HA column using buffer F [500 mM potassium phosphate, 20% glycerol, and 0.1 mM DTT (pH 7.5)] at a flow rate of 9 mL h^{-1}. The pooled fractions were dialyzed overnight against 2 L of buffer G [10 mM potassium phosphate, 20% glycerol, 1 mM EDTA, and 0.1 mM DTT (pH 7.5)] and aliquoted and stored at −70 °C until they were used. The specific content of the final preparations was typically ≥14 nmol of P450 (mg of protein)$^{-1}$.

7-(Benzyloxy)resorufin and 7-(Pentyloxy)resorufin O-Dealkylase Assays. 7-(Benzyloxy)resorufin and 7-(pentyloxy)resorufin *O*-dealkylase activities of the P450 2B1 wild type and mutants were examined in a reconstituted system as described earlier (*8*), using purified P450 preparations. Formation of resorufin was monitored flourometrically using an excitation wavelength of 550 nm and an emission wavelength of 585 nm (*8*).

7-Alkoxycoumarin Dealkylase Assays. The reconstituted protein system contained 10 pmol of purified P450 enzyme, 20 pmol of recombinant NADPH−cytochrome P450 reductase, and 30 μg mL^{-1} DLPC and was incubated for 10 min at room temperature prior to the addition of 20 pmol of rat liver cytochrome b_5. Alkoxycoumarin substrate (300 μM) was dissolved in methanol and the mixture added to the reconstituted protein system in 50 mM HEPES buffer (pH 7.6). After incubation for 5 min at 37 °C, product formation was measured as described (*24*).

Stoichiometry Measurements. To measure 7-hydroxycoumarin formation, NADPH oxidation, oxygen consumption, and hydrogen peroxide production from 7-butoxycoumarin, a reaction mixture was prepared as described (*24*) with some modifications. The reconstituted system contained 2.5 μM P450 2B1 V363A or V363L, 5.0 μM NADPH−cytochrome P450 reductase, and 30 μg mL^{-1} DLPC and was equilibrated at room temperature for 10 min prior to the addition of 5.0 μM rat liver cytochrome b_5. The final reaction mixture contained 0.05 μM P450, 0.1 μM NADPH−cytochrome P450 reductase, 0.1 μM cytochrome b_5, 300 μM 7-butoxycoumarin, 15 mM $MgCl_2$, 30 μg mL^{-1} DLPC, 0.2 mM NADPH, and 50 mM HEPES (pH 7.6). The reaction was initiated by adding the reconstituted enzymes and quenched after incubation for 10 min at 37 °C by adding $^1/_{10}$ volume of 0.5 M sulfuric acid. The rates of NADPH oxidation, H_2O_2 production, and 7-hydroxycoumarin formation were measured from the same reaction, as described previously for 7-ethoxycoumarin (*24*).

Identification of 7-Butoxycoumarin Metabolites Produced by E. coli-Expressed Purified 2B1 Wild Type and V363A and V363L Mutants Using HPLC and GC−EIMS. To obtain sufficient quantities of products, a large scale incubation of P450 proteins with 7-butoxycoumarin was conducted. The composition of the reconstituted system was the same as described above, except that the concentration of the substrate was 400 μM rather than 300 μM, according to the method of Reen et al. (*9*). In the case of incubation with phenobarbital-treated rat liver microsomes, the reaction mixture contained 0.5 mg mL^{-1} microsomal proteins. 7-Butoxycoumarin metabolites were extracted with chloroform in the same manner as previously described (*24*) after adding hydrochloric acid. The chloroform phase was then evaporated under a stream of nitrogen gas at 37 °C to obtain the dried residue for further analyses using HPLC and GC−EIMS.

For HPLC analyses, an ultrasphere ODS column (5 μm × 250 mm × 4.6 mm, Beckman, Fullerton, CA) was used with an ultrasphere C18 guard column (5 μm × 7.5 mm × 4.6 mm, Alltech, Deerfield, IL). The column was eluted isocratically with a mobile phase of 10 mM acetate buffer (pH 3.6)/methanol/tetrahydrofuran (60:32:8, v/v/v). The flow rate was 1.0 mL min^{-1}, and the UV detector was set at 330 nm. All HPLC separations were performed at room temperature, and dried extracts were dissolved in the mobile phase before being injected onto the column.

Prior to GC−EIMS analyses, 7-butoxycoumarin metabolites were separated by TLC. The chloroform extracts obtained from 2−4 mL enzymatic reaction mixtures were dissolved in ethyl acetate and applied onto a silica gel TLC

plate (Baker Si250). The plate was developed with benzene/ethyl acetate (80:20, v/v) as described by Reen et al. (*9*), and products were detected by their fluorescence under ultraviolet light. The fluorescent TLC bands were scraped, and the metabolites were extracted three times with 2 mL of methanol. The solvent was subsequently evaporated under a stream of nitrogen gas at 37 °C. Dried TLC extracts were dissolved in 20 μL of ethyl acetate, and 1−3 μL of the sample was used for product identification on a Hewlett-Packard GC−MS system (Palo Alto, CA). Products were introduced by splitless injection and separated on a 30 m DB5MS fused-silica capillary column (0.25 mm inside diameter, 0.25 μm film). The temperature of the column was held at 70 °C for 1 min, raised to 230 °C at a rate of 30 °C min^{-1} and then to 280 °C at a rate of 5 °C min^{-1}, and maintained at 280 °C for 3 min. The carrier gas was helium, with a head pressure of 135 Kpag.

Computer Modeling. The model of P450 2B1 was constructed previously (*16*), and the crystal structure of 7-ethoxycoumarin (*34*) was obtained from the Cambridge Structural Database. The structures of 7-propoxy- and 7-butoxycoumarin were constructed by modifying the structure of 7-ethoxycoumarin using the Builder module of the InsightII modeling package (Biosym/MSI, San Diego, CA). The three-dimensional structures were displayed on a Silicon Graphics workstation with InsightII. Energy minimization and molecular dynamics simulations were carried out with the Discover program, version 2.97 (Biosym/MSI), using the consistent valence force field. The parameters for heme and ferryl oxygen were as described by Paulsen and Ornstein (*35*, *36*).

Each of the substrates, i.e., 7-ethoxy-, 7-propoxy-, and 7-butoxycoumarin, was docked into the P450 2B1 active site in a reactive binding orientation, leading to alkoxycoumarin dealkylation. The initial oxidation step involves hydrogen abstraction at the side chain carbon bonded to the oxygen of the alkoxy group. Therefore, the C1 atom of the alkyl chain was placed 3.7 Å from ferryl oxygen, with one of the hydrogen atoms bonded to C1 directed toward ferryl oxygen (C−H−ferryl O angle of 180°) to promote hydrogen bond formation. 7-Butoxycoumarin was also docked in two other orientations, leading to ω or $\omega - 1$ hydroxylation. In these cases, the carbon atom to be hydroxylated was C4 or C3 of the alkyl chain, respectively.

For all substrates and binding orientations, enzyme−substrate interactions were optimized with molecular dynamics. In these simulations, the carbon atom to be oxidized and the hydrogen atom to be abstracted were fixed, while the rest of the alkoxycoumarin molecule, along with the side chains of protein residues within 5 Å of the substrate, was allowed to move (*37*, *38*). Initially, the system was minimized using the steepest descent method and harmonic potential, with a nonbond cutoff of 10 Å, to a maximum gradient of 5 kcal mol^{-1} Å^{-1}. Molecular dynamics simulations followed by energy minimization were performed as described (*37*, *38*). Briefly, the system was equilibrated for 0.1 ps, and the simulations were continued for 1 ps at 300 K using 1 fs time steps. After conjugate gradient minimization, the nonbond interaction energy between the substrate and the protein was evaluated with the Docking module of InsightII.

Table 1: 7-(Benzyloxy)resorufin and 7-(Pentyloxy)resorufin *O*-Dealkylase Activities of the *E. coli*-Expressed Purified 2B1 Wild Type and Five Site-Directed Mutants[a]

P450 enzyme	(benzyloxy)resorufin	(pentyloxy)resorufin
rat 2B1[b]	11.09 (87)	3.72 (83)
wild type	12.75 (100)	4.50 (100)
I114V	5.05 (40)	2.60 (58)
F206L	1.63 (13)	0.79 (18)
V363A	3.67 (29)	1.64 (36)
V363L	7.62 (60)	1.60 (36)
G478S	0.73 (6)	0.36 (8)

[a] Values are derived from duplicate incubations performed as described in Experimental Procedures. [b] Refers to 2B1 purified from rat liver. Activities are expressed in nanomoles of product per minute per nanomole of P450. Numbers in parentheses represent the rate as a percentage of the *E. coli*-expressed purified P450 2B1 wild-type rate.

RESULTS

7-(Benzyloxy)resorufin and 7-(Pentyloxy)resorufin O-Dealkylase Activities. To confirm the functional integrity of the recombinant proteins, experiments were conducted using (benzyloxy)- and (pentyloxy)resorufins as substrates. As shown in Table 1, the catalytic activities of purified *E. coli*-expressed and the rat hepatic P450 2B1 were very similar. Moreover, O-dealkylation rates of the two substrates for purified wild-type and mutant recombinant enzymes were approximately 2-fold higher than for the CHAPS-solubilized membrane preparations (data not shown). All the 2B1 mutants studied exhibited activities lower than that of the wild-type enzyme, ranging from 60% (V363L mutant) to 6% (G478S mutant) for 7-(benzyloxy)resorufin and from 58% (I114V mutant) to 8% (G478S mutant) for 7-(pentyloxy)-resorufin (Table 1). The pattern of (benzyloxy)resorufin oxidation by the wild-type and mutant enzymes was similar to that observed with (pentyloxy)resorufin as a substrate.

Alkoxycoumarin O-Dealkylase Activities. Panels A and B of Figure 1 show alkoxycoumarin *O*-dealkylase activities of the P450 2B1 wild type and five mutants as a function of the length of the alkyl chain. The wild-type enzyme exhibited the highest activity with 7-ethoxycoumarin as a substrate, followed by butoxycoumarin, propoxycoumarin, and methoxycoumarin (Figure 1A). The pattern of alkoxycoumarin O-dealkylation by the purified rat hepatic P450 2B1 was the same as that observed with the *E. coli*-expressed enzyme (data not shown). P450 2B1 V363L also showed a preference for 7-ethoxycoumarin as a substrate with activity similar to that of the wild-type enzyme. Thereafter, the activity of the mutant declined sharply with increasing length of the alkyl chain, reaching a minimum for 7-butoxycoumarin. On the other hand, the pattern of alkoxycoumarin O-dealkylation by 2B1 V363A was strikingly different. The rate of substrate oxidation increased gradually with increasing length of the alkyl chain, reaching a maximum for 7-butoxycoumarin, and decreased gradually for alkoxycoumarins with a chain length of 5−7 carbon atoms.

Alkoxycoumarin *O*-dealkylase activities of P450 2B1 I114V, F206L, and G478S mutants are shown in Figure 1B. The pattern of substrate O-dealkylation by I114V was very similar to that observed for the wild-type enzyme. No differences were detected among various alkoxycoumarins with G478S, which exhibited very low activities with all the compounds (Figure 1B). F206L showed the highest activity

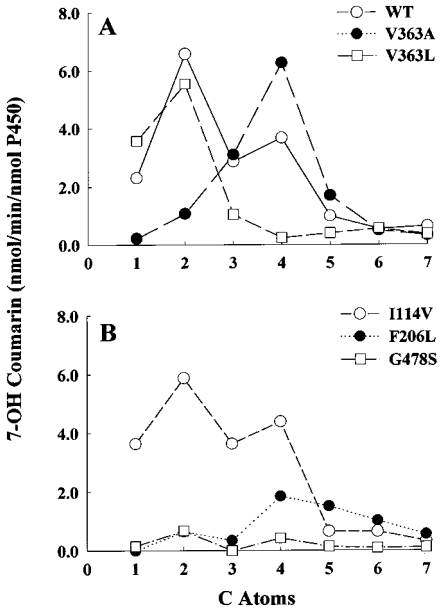

FIGURE 1: Effect of chain length on the oxidation of 7-alkoxycoumarin by purified recombinant P450 wild type and five active site mutants. The 0.75 mL reaction mixture contained 10 pmol of purified enzyme, 20 pmol of NADPH−cytochrome P450 reductase, 10 pmol of rat hepatic cytochrome b_5, and 300 μM substrate. Other experimental conditions and details are described in Experimental Procedures.

Table 2: O-Dealkylation of 7-Isobutoxycoumarin and 7-Neobutoxycoumarin by the *E. coli*-Expressed Purified P450 2B1 Wild Type and V363A and V363L Mutants[a]

P450 enzyme	7-isobutoxycoumarin	7-neobutoxycoumarin
wild type	2.32	0.16
V363A	10.19	1.17
V363L	ND[b]	ND

[a] Values are derived from duplicate incubations performed as described in Experimental Procedures. Activities are expressed in nanomoles of product per minute per nanomole of P450. [b] ND, not detectable.

with 7-butoxycoumarin, but the rate of O-dealkylation gradually decreased upon further extension of the alkyl chain (Figure 1B). In conclusion, the most striking alterations in activity toward alkoxycoumarins as a function of chain length were observed when Val-363 was replaced with Leu or Ala.

O-Dealkylation of Other Coumarin Derivatives. To explore further the effect of the alkyl side chain on catalysis, two additional compounds were tested as substrates for the wild-type enzyme and Val-363 mutants. As shown in Table 2, *O*-dealkylase activities of V363A with 7-isobutoxycoumarin and 7-neobutoxycoumarin were 4.4- and 7.3-fold higher, respectively, than those of the wild-type enzyme. In contrast, the activities of the V363L mutant were undetectable. Thus, the trend observed with 7-butoxycoumarin as a substrate (Figure 1A) also held true for the structural analogues of this compound having branched alkyl chains.

Stoichiometry of 7-Butoxycoumarin Oxidation by P450 2B1 V363A and V363L Mutants. To elucidate further the function of the amino acid residue at position 363 in cytochrome P450 2B1, the stoichiometry of 7-butoxycoumarin oxidation by P450 2B1 V363A and V363L was examined. The rates of NADPH oxidation, oxygen consumption, 7-hydroxycoumarin formation, hydrogen peroxide formation, and excess water production are presented in Table 3. Because of rapid dismutation of superoxide to H_2O_2 (*24*), measurements of hydrogen peroxide formation served as an indicator of dissociation of oxygen from the $[FeO_2]^{2+}$-RH or $[FeO_2H]^{2+}$-RH intermediates. The rates of excess water formation were calculated from (1) the difference between the rate of NADPH oxidation and rates of hydrogen peroxide and 7-hydroxycoumarin formation and (2) the difference between the rate of NADPH oxidation and the rate of oxygen consumption (*24*). The latter calculation does not require prior knowledge of product formation during the reaction. The extent of uncoupling of reducing equivalents to hydrogen peroxide at the $[FeO_2]^{2+}$-RH or $[FeO_2H]^{2+}$-RH intermediate branch points was assessed from the ratio of hydrogen peroxide production to oxygen consumption (*20*), as shown in Table 3. The extent of uncoupling to water at the level of the $[FeO]^{3+}$-RH intermediate was assessed from the ratio of excess water formation at that branch point to the formation rate of the $[FeO]^{3+}$-RH intermediate. The latter was calculated from the difference between oxygen consumption and hydrogen peroxide production.

The extent of uncoupling to water was higher for V363A than for the V363L (Table 3). However, the ratio of 7-hydroxycoumarin formation to NADPH consumption for the V363L mutant was much smaller than that for V363A. These results suggested that metabolites other than 7-hydroxycoumarin must be produced from 7-butoxycoumarin by V363L. That conclusion is further supported by the fact that excess water formation by V363L calculated from eq 1 was twice as high as that obtained from eq 2 (Table 3). In contrast, the corresponding values were in close agreement for the V363A mutant. To further confirm the formation of other 7-butoxycoumarin metabolites, HPLC analysis was performed.

Oxidation of 7-Butoxycoumarin by E. coli-Expressed Purified P450 2B1 Wild Type and V363A and V363L Mutants. HPLC chromatograms of 7-butoxycoumarin metabolites produced by the 2B1 wild type and V363A and V363L mutants are depicted in Figure 2. The wild-type enzyme and rat liver microsomes produced 7-hydroxycoumarin, which eluted at 6.78 min, and two unknown metabolites. The major one (M1) eluted at 15.07 min, and the minor metabolite (M2) eluted at 12.73 min. These results are in agreement with those of Reen et al. (*9*), who reported that phenobarbital-treated Sprague-Dawley rat liver microsomes metabolized 7-butoxycoumarin to yield not only 7-hydroxycoumarin but also two additional metabolites. In our experiments, the amount of the M1 product seemed to be lower than that of 7-hydroxycoumarin, while the level of M2 was very low (Figure 2). Interestingly, for the V363A mutant, M1 was a minor metabolite and M2 was not detected. In contrast, the major metabolite produced from 7-butoxycoumarin by the V363L mutant was M1, with minor amounts of M2 and 7-hydroxycoumarin. Thus, substitutions at position 363 of P450 2B1 had a profound effect on product distribution. The presence of Ala at this position yielded 7-hydroxycoumarin as the major product of 7-butoxycoumarin oxidation, while the presence of Leu greatly favored M1 production. Since the identities of additional 7-butoxycoumarin metabolites have not been determined (*9*), we proceeded with their identification using GC−EIMS.

Table 3: Stoichiometry of 7-Butoxycoumarin Oxidation Catalyzed by *E. coli*-Expressed P450 2B1 V363A and V363L Mutants[a]

2B1 enzyme	NADPH oxidation	O_2 consumption	product formation	H_2O_2 production	water formation		7-hydroxycoumarin/ NADPH[b]	H_2O_2/O_2[b]	H_2O[c]/ ($O_2-H_2O_2$)
					eq 1	eq 2			
V363A	32 ± 4.0	21.5 ± 1.2	5.9 ± 0.2	4.6 ± 1.0	21	21	0.18	0.21	0.62
V363L	158 ± 3.0	127 ± 6.0	0.5 ± 0.0	22.2 ± 1.4	135	62	0.003	0.17	0.30

[a] Values represent the mean ± SD from triplicate incubations performed as described in Experimental Procedures. Activities are expressed in nanomoles of product per minute per nanomole of P450. Reaction mixtures contained 0.05 μM P450, 0.10 μM NADPH−cytochrome P450 reductase, and 0.10 μM cytochrome b_5 and were incubated for 10 min at 37 °C. Equation 1 is $[H_2O]_{excess} = [NADPH]_{oxidized} - [7\text{-OH-coumarin}]_{formed} - [H_2O_2]_{produced}$. Equation 2 is $[H_2O]_{excess} = 2([NADPH]_{oxidized} - [O_2]_{consumed})$. [b] Expressed as ratios of rates. [c] H_2O formed in the uncoupling step, which equals half of the excess water formation calculated with the equation $[H_2O]_{excess} = 2([NADPH]_{oxidized} - [O_2]_{consumed})$.

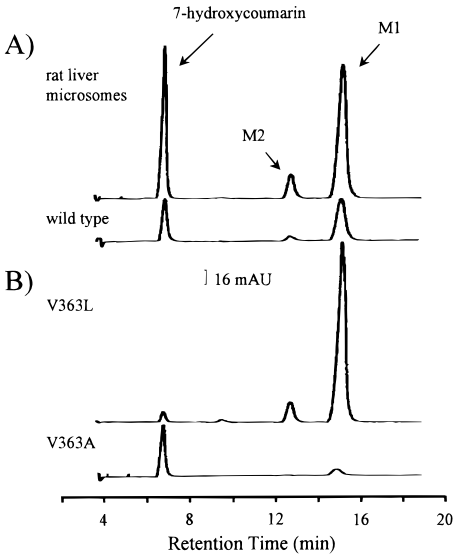

FIGURE 2: HPLC chromatograms of 7-butoxycoumarin metabolites: (A) P450 2B1 wild type and rat liver microsomes and (B) P450 2B1 V363A and V363L mutants. The metabolites of 7-butoxycoumarin, i.e., 7-(3-hydroxy)-butoxycoumarin and 7-(4-hydroxy)-butoxycoumarin are shown as M1 and M2, respectively. Experimental conditions are described in "Experimental Procedures".

Identification of 7-Butoxycoumarin Metabolites. A relatively large scale incubation of 7-butoxycoumarin with phenobarbital-induced rat liver microsomes was performed, and the metabolites were separated by TLC and subjected to GC−EIMS analysis. The peaks obtained from GC were correlated with those from HPLC by spiking HPLC samples with a given TLC-purified metabolite. The M1 product had an R_f value of 0.13 on TLC and cochromatographed with authentic 7-(3-hydroxybutoxy)coumarin ($\omega - 1$ hydroxylation), while M2 had an R_f value of 0.10 on TLC and cochromatographed with 7-(4-hydroxybutoxy)coumarin (ω hydroxylation). The total ion gas chromatograms and electron impact mass spectra of M1 and M2 are shown in Figure 3. Both metabolites were identified as monohydroxylated butoxycoumarin compounds as indicated by their molecular ion peaks ($M^+ = m/z$ 234). On the basis of mass spectral analysis, the metabolite M2 with the GC retention time of 12.87 min was ω-hydroxylated 7-butoxycoumarin. The characteristic peaks for the metabolite were m/z 234, 162, and 134, and according to this pattern, a fragmentation scheme was proposed in Figure 3A. The identity of the metabolite was confirmed by comparison with the GC retention time and mass spectrum of the standard (data not shown). The analysis of the mass spectrum of the metabolite M1 with the GC retention time of 11.97 min indicated that this was $\omega - 1$-hydroxylated butoxycoumarin.

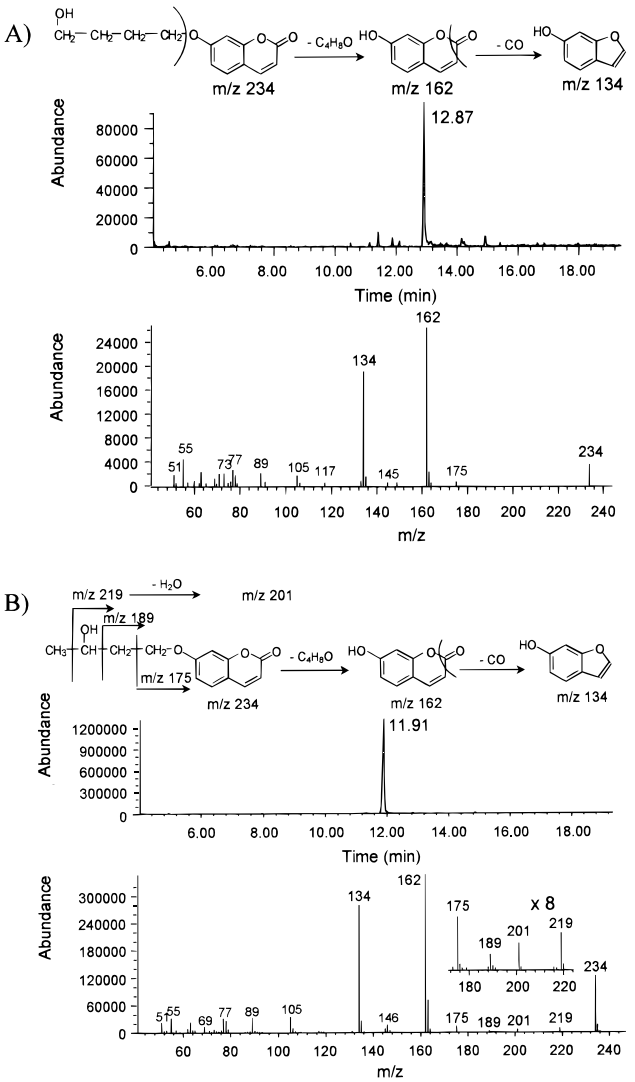

FIGURE 3: Total ion gas chromatograms and electron impact mass spectra of 7-butoxycoumarin metabolites with R_f values on TLC of 0.10 (A) and 0.13 (B).

This metabolite showed major fragmentation peaks at m/z 234, 162, and 134, like those obtained from ω-hydroxylated 7-butoxycoumarin. However, several other characteristic peaks were present with m/z 219, 201, and 189 (Figure 3B inset). These peaks were not detected in the mass spectrum of M2 (Figure 3A) and were assigned to decomposed fragments of $\omega - 1$-hydroxylated 7-butoxycoumarin in the gas phase, as proposed in Figure 3B. The identity of the metabolite was confirmed by cochromatography on GC with the standard and by comparison of the mass spectra (data not shown).

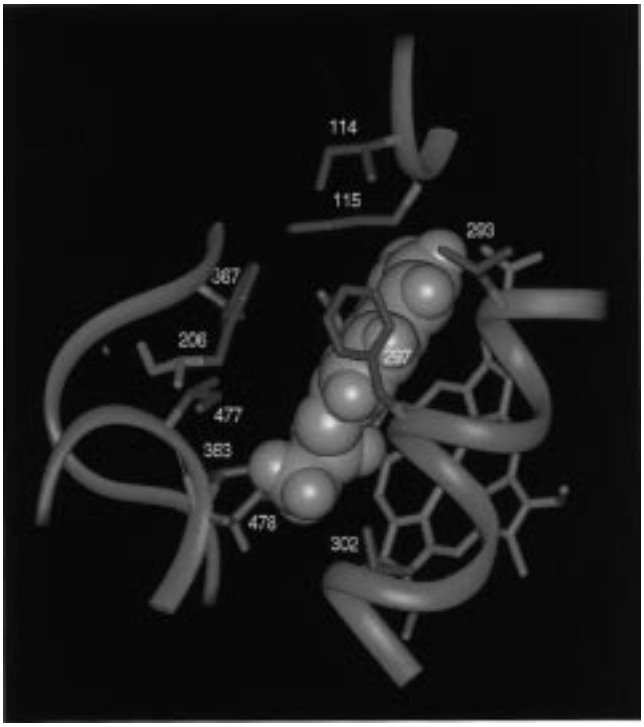

FIGURE 4: 7-Ethoxycoumarin docked into the active site of a cytochrome P450 2B1 model in an orientation allowing for O-deethylation. The substrate is shown in yellow, with all hydrogens displayed. Heme is shown in red. Key residues of 2B1 enzyme (114, 206, 363, and 478) are located within 5 Å of 7-butoxycoumarin. When Gly-478 is replaced with Ser (green), van der Waals overlaps are observed between the side chain of Ser and the substrate.

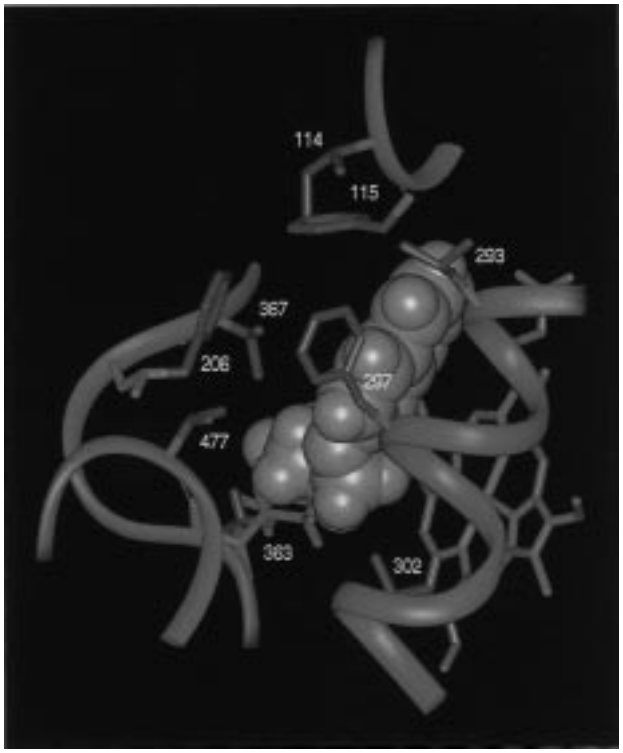

FIGURE 5: 7-Butoxycoumarin docked into the P450 2B1 V363A mutant in an orientation allowing for substrate O-dealkylation. The substrate is shown in yellow, with all hydrogens displayed. Heme is shown in red. Ala at position 363 (magenta) allows the substrate to assume the orientation allowing for its debutylation, while the larger Val would create van der Waals overlaps with the substrate.

Molecular Modeling. To explain changes in activity observed during oxidation of various alkoxycoumarins by P450 2B1 and mutants, molecular modeling was used. Figure 4 shows 7-ethoxycoumarin docked in the active site of the P450 2B1 model in an orientation leading to O-dealkylation. Residues 363 and 478 are within 4 Å of the substrate and may directly interact with the alkoxycoumarin side chain. Residues 114 and 206, which also constitute part of the active site, are farther from the substrate. Phe-206 is within 5 Å, while Ile-114 is found within 6 Å. Moreover, residue 114 is screened from the substrate by other residues, in particular 297, and thus cannot directly interact with the alkoxycoumarins bound in the active site in the orientation leading to O-dealkylation. 7-Ethoxycoumarin fits well into the 2B1 active site with no van der Waals overlaps. However, the increased length of the alkyl chain leads to overlaps between the substrate and the enzyme, mainly with residues 363 and 478. For example, 7-propoxycoumarin shows a 0.3 (30%) overlap between the atoms of its terminal methyl group and the side chain of Val-363, while 7-butoxycoumarin displays a 0.4 overlap with this residue. Modeling results are thus consistent with the experimentally observed decrease in dealkylation rates for these substrates (Figure 1A). Similarly, 7-isobutoxycoumarin and 7-neobutoxycoumarin were difficult to dock into the P450 2B1 active site because of steric hindrance due to the bulky alkyl chain bound to the coumarin skeleton (not shown), in agreement with experimental results (Table 2).

In the P450 2B1 G478S mutant, van der Waals overlaps (0.2 overlap) occur between 7-ethoxycoumarin and the side chain of Ser, which might prevent substrate O-dealkylation (Figure 4). These overlaps are also present, and to a larger extent, with alkoxycoumarins containing alkyl chains longer than 2 carbon atoms, as indicated also by the increased interaction energy between the enzyme and the substrate. For 7-propoxycoumarin, overlaps of up to 0.5 are observed with the Ser-478 side chain. In the case of 7-butoxycoumarin, steric hindrance is compounded by the presence of additional van der Waals overlaps with resides 363 and 367 (not shown). This might explain the very low *O*-dealkylase activity of the G478S mutant toward alkoxycoumarins (Figure 1).

7-Butoxycoumarin can be docked in the V363A mutant in an orientation allowing its O-dealkylation (Figure 5). The Ala side chain is small enough to permit bending of the butoxy chain, which is not possible in the wild-type enzyme due to van der Waals overlaps with Val-363. At the same time, the presence of Ala at position 363 leads to increased mobility of smaller alkoxycoumarins, such as 7-ethoxy- and 7-propoxycoumarin, consistent with lowered *O*-dealkylase activities (Figure 1A). Extending the length of the alkoxy chain more than 4 carbon atoms causes van der Waals overlaps with other residues in the active site, such as 367 (data not shown).

In contrast to V363A, the presence of a larger Leu at position 363 did not allow for binding of 7-propoxy- or 7-butoxycoumarin in an orientation leading to O-dealkylation. Significant van der Waals overlaps between the substrate and the Leu side chain were observed: a 0.3 overlap in the case of 7-propoxycoumarin and an up to 0.6−0.7 overlap in the case of 7-butoxycoumarin. These values are much larger than those observed in the wild-type enzyme.

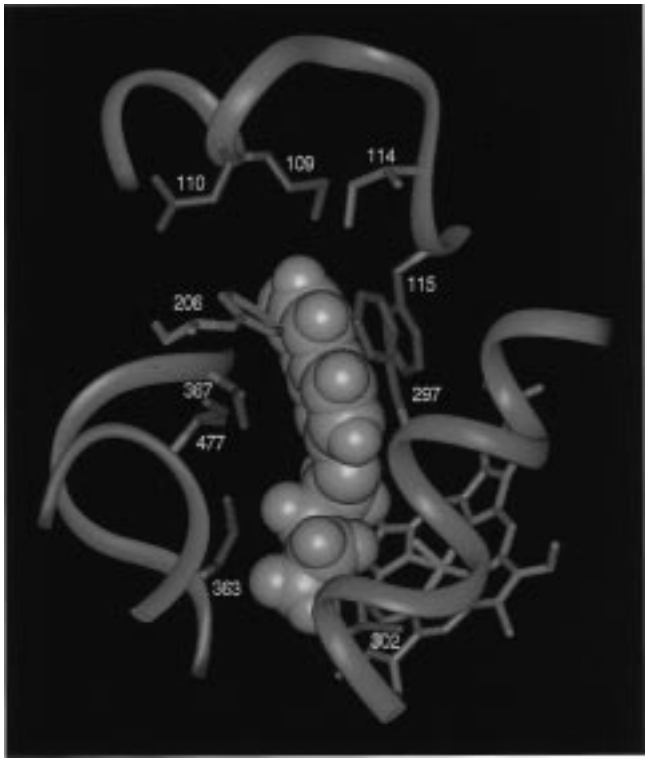

FIGURE 6: 7-Butoxycoumarin docked into the P450 2B1 V363L mutant in an orientation leading to substrate $\omega - 1$ hydroxylation. The substrate is shown in yellow, with all hydrogens displayed. Heme is shown in red. Leu-363 stabilizes the binding of the substrate in this orientation.

However, the presence of this large residue allowed binding of 7-butoxycoumarin in alternate orientations, resulting in ω and $\omega - 1$ hydroxylation of the alkoxy chain. Figure 6 shows 7-butoxycoumarin docked into the active site of the P450 2B1 V363L mutant in an orientation allowing for its $\omega - 1$ hydroxylation, with the substrate now positioned closer to residues 114 and 206 (within 4 Å) in the upper part of the binding pocket. In summary, molecular modeling results were remarkably consistent with experimental data and allowed us to explain changes in the metabolism of alkoxycoumarins by various P450 2B1 mutants.

DISCUSSION

The O-dealkylation of 7-ethoxycoumarin has been routinely used to detect P450 activity (*29*), and alkoxycoumarins with alkyl chains of different lengths have been employed to discriminate among different P450 isoforms (*9*, *25*, *31*). Our current studies represent the first attempt to evaluate these compounds as specific probes for exploring the active site of a single enzyme, P450 2B1. We investigated the oxidation of 7-alkoxycoumarins with a chain length of 1−7 carbon atoms by purified *E. coli*-expressed P450 2B1 wild type and five site-directed mutants (I114V, F206L, V363A, V363L, and G478S). A combination of approaches, including stoichiometry measurements, novel metabolite identification, and molecular modeling, was used to examine the architecture of the substrate binding pocket, in particular its size and the role of key residues in determining enzyme−substrate interactions.

The ability of wild-type P450 2B1 to oxidize specific alkoxycoumarins was found to depend on the length of the alkyl chain of the substrate. The enzyme preferentially metabolized 7-ethoxycoumarin, and decreased or increased length or branching of the alkyl chain led to a decrease in substrate O-dealkylation. Molecular modeling indicated that van der Waals overlaps occur between active site residues (especially 363 and 478) and the substrate alkyl chain when it is longer than 2 carbon atoms. In contrast, the lower rate of 7-methoxycoumarin O-demethylation may be due to increased mobility of the substrate. 7-Ethoxycoumarin appears to fill the active site of the enzyme optimally. The role of particular active site residues in substrate binding and oxidation was examined further using selected site-directed mutants.

The pattern of O-dealkylation of various alkoxycoumarins by 2B1 I114V was very similar to that of the wild-type enzyme. On the basis of molecular modeling, this residue is farther than 5 Å from the bound substrate and screened by other active site residues; thus, it cannot directly interact with alkoxycoumarins. Moreover, our recent studies on the stoichiometry of 7-ethoxycoumarin oxidation have shown that the efficiency of coupling of reducing equivalents to 7-hydroxycoumarin formation was unchanged for I114V (*24*). This lack of effect of the Ile-114 → Val substitution is in contrast to results obtained with other substrates. For example, greatly increased hydroxylation rates of progesterone were observed with P450 2B1 I114V, while androstenedione was oxidized less rapidly and exhibited altered regiospecificity compared with the wild type (*7*, *8*). The activities of the mutant toward (benzyloxy)- and (pentyloxy)-resorufin were much lower (*8*), as confirmed in these studies.

P450 2B1 F206L was characterized by very low rates of alkoxycoumarin O-dealkylation compared with that of the wild type, although extending the length of the alkyl chain to 4 carbon atoms increased enzymatic activity. This residue is within 5 Å of the 7-ethoxycoumarin substrate, so the substitution of Phe with the smaller and more flexible Leu (the volume of Phe is about 190 $Å^3$, while that of Leu is 167 $Å^3$) may increase the volume of the active site and lead to excessive substrate mobility. This reasoning is supported by the decrease in coupling of NADPH to product formation during oxidation of 7-ethoxycoumarin by F206L, which is accompanied by increased uncoupling to water (*24*). Consequently, increased activity of F206L with coumarins having longer alkyl chains (4 carbons or more) is probably due to better binding of these bigger substrates in the enlarged active site. The replacement of Phe-206 by Leu in P450 2B1 also affected steroid hydroxylation, decreasing overall activity and altering product profiles with androstenedione and testosterone, while progesterone oxidation was increased (*7*, *8*). The activities with (benzyloxy)- and (pentyloxy)resorufin were lower than that for the wild type (Table 1 and ref *8*), although benzphetamine N-oxidation was not affected (*8*).

The replacement of Gly-478 with Ser in P450 2B1 greatly decreased the O-dealkylation of alkoxycoumarins in an alkyl chain length-independent manner. Molecular modeling indicated that the decrease in activity may be due to van der Waals overlaps between the substrate and the Ser side chain. However, it is also possible that the introduction of a hydrophilic side chain may have an effect on the local conformation of the pocket or on interactions with other active site residues. In the case of 7-methoxycoumarin, no van der Waals overlaps are observed between the substrate

and Ser-478 (data not shown), and thus, other factors must be responsible for low levels of O-demethylation. Steric hindrance, however, was observed with larger substrates, including 7-ethoxycoumarin. This is in agreement with stoichiometry measurements of 7-ethoxycoumarin O-deethylation, which revealed decreased coupling of NADPH to product formation and increased uncoupling to water (*24*). The side chain of residue 478 was previously found to be a major determinant of steroid oxidation, altering regio- and stereospecificity of androstenedione (*4*, *5*) and testosterone (*5*) hydroxylation. Moreover, the G478S mutant was characterized by low rates of product formation from androstenedione and progesterone (*8*), as well as from (benzyloxy)- and (pentyloxy)resorufin (Table 1 and ref *8*), compared with that of the wild-type enzyme. Thus, residue 478 is of major importance for substrate oxidation by P450 2B1, but in the case of alkoxycoumarins, the effect of its replacement is so drastic and uniform that the utility of these compounds as probes of the active site architecture is compromised.

A quite different phenomenon is observed with residue 363 in P450 2B1. When Val-363 was replaced with either Ala or Leu, different effects on alkoxycoumarin oxidation were seen, depending on the length and branching of the alkyl chain. With V363A, the increase in the volume of the active site allows a larger substrate, such as 7-butoxycoumarin, to bind in an orientation leading to O-dealkylation. In fact, the mutant enzyme displayed the highest activity with that compound, as well as high coupling to 7-hydroxycoumarin formation. Likewise, 7-butoxycoumarin analogues with branched alkyl chains are likely to fit better into the active site of the mutant than into the wild-type enzyme, explaining their increased O-dealkylation. Substrates smaller than 7-butoxycoumarin can exhibit higher mobility in the active site, while compounds with an alkyl chain longer than 4 carbon atoms may encounter van der Waals overlaps, in both cases resulting in lowered activity. Studies of the stoichiometry of 7-ethoxycoumarin metabolism showed that V363A displayed reduced coupling to product and increased uncoupling to water (*24*), consistent with increased substrate mobility. In the case of V363L, the highest *O*-dealkylase activity was observed with 7-ethoxycoumarin, and the rates decreased rapidly upon extension of the coumarin alkyl chain beyond 2 carbon atoms. The activity toward branched chain analogues was undetectable. Since residue 363 can directly interact with the substrate, the presence of a large Leu residue may interfere with binding of larger alkoxycoumarins in an orientation allowing for their O-dealkylation, as indicated by the appearance of van der Waals overlaps. The role of residue 363 in regio- and stereospecificity of substrate oxidation by P450 2B enzymes has been reported previously (*7*, *8*, *14*, *18*), and these studies provide further support for the importance of this residue in enzyme catalysis. With alkoxycoumarins as substrates, the *O*-dealkylase activity is largely determined by the size of the amino acid residue at position 363.

An interesting phenomenon observed with the P450 2B1 V363L mutant was the metabolic switching with 7-butoxycoumarin as a substrate. This was initially indicated by stoichiometry measurements, which showed that the rate of excess water production calculated from the equation containing a term for 7-hydroxycoumarin product formation was much higher than the value independent of product formed. Additional metabolites were then identified by GC−EIMS. In contrast to the wild-type enzyme, O-dealkylation of 7-butoxycoumain by V363L was almost abolished, and the major product was $\omega - 1$-hydroxylated butoxycoumarin. The increased size of the side chain at position 363 of 2B1 seems to "push" the substrate into an alternate orientation. Interestingly, these new metabolites were not observed in the V363A mutant, possibly due to increased mobility of 7-butoxycoumarin in the active site of that mutant. Harada et al. (*39*) using deuterated 7-ethoxycoumarin detected the formation of a second metabolite, 6-hydroxy-7-ethoxycoumarin, arising from the metabolic switching from the *O*-ethyl group to the aromatic ring of this substrate. In our studies, we did not observe ring hydroxylation with the 2B1 wild type or 363 mutants using 7-butoxycoumarin as a substrate. However, alkyl side chain hydroxylation at ω and the $\omega - 1$ positions was detected in the V363L mutant, as well as in the wild-type enzyme.

The possibility of metabolic switching in the V363L mutant raises the interesting question of whether side chain hydroxylation of alkoxycoumarins follows the rule small substrate + bulky 363 residue = bulky substrate + small 363 residue. In the case of 7-ethoxycoumarin and the V363L mutant, only dealkylation was observed. This is perhaps not surprising since the thermodynamically favored $\omega - 1$ reaction leads to ether cleavage with the ethoxy compound. In contrast, the results of preliminary studies using V363A and 7-pentoxy-, 7-hexoxy-, and 7-heptoxycoumarin show that side chain hydroxylation products are formed, as observed on TLC. The extent of ether cleavage by V363A diminishes and the extent of side chain hydroxylation increases with increasing length of the alkyl chain from C5 to C7 (data not shown).

As shown in this investigation, alkoxycoumarins can be utilized as sensitive probes of the active site architecture of P450 2B enzymes. Our previous studies employed mainly steroids, which were very sensitive to key residue replacement, with many mutants exhibiting altered regio- or stereospecificity of substrate hydroxylation. However, with alkoxycoumarins, it was possible to discern a relationship between the size of the active site and the length of the alkyl chain of the substrate, as demonstrated with 2B1 residue 363 mutants. Moreover, we have demonstrated the advantages of a comprehensive approach to studying the function of particular amino acid residues that involved biochemical assays, stoichiometry measurements, and molecular modeling. This combination of techniques can be utilized to study other P450 enzymes and thus provide deeper insight into cytochrome P450 structure−function relationships.

ACKNOWLEDGMENT

Molecular modeling studies were performed at the Molecular Modeling Facility of the Southwest Environmental Health Sciences Center (SWEHSC) at The University of Arizona (Tucson, AZ). Butoxycoumarin metabolite standards were synthesized by Dr. Steve Waller and Dr. James Baron (Department of Chemistry, The University of Arizona). The authors thank Dr. Greg R. Harlow for helpful discussions.

REFERENCES

1. Lu, A. Y. H., and West, S. B. (1980) *Pharmacol. Rev. 31*, 277−295.
2. Guengerich, F. P. (1987) in *Progress in Drug Metabolism* (Bridges, J. W., Chasseaud, L. F., and Gibson, G. G., Eds.) Vol. 10, pp 1−54, Taylor & Francis, London.
3. Guengerich, F. P. (1993) *Drug Metab. Dispos. 21*, 1−6.
4. Kedzie, K. M., Balfour, C. A., Escobar, G. Y., Grimm, S. W., He, Y. A., Pepperl, D. J., Regan, J. W., Stevens, J. C., and Halpert, J. R. (1991) *J. Biol. Chem. 266*, 22515−22521.
5. He, Y. A., Balfour, C. A., Kedzie, K. M., and Halpert, J. R. (1992) *Biochemistry 31*, 9220−9226.
6. Halpert, J. R., and He, Y. A. (1993) *J. Biol. Chem. 268*, 4453−4457.
7. He, Y. A., Luo, Z., Klekotka, P. A., Burnett, V. L., and Halpert, J. R. (1994) *Biochemistry 33*, 4419−4424.
8. He, Y. Q., He, Y. A., and Halpert, J. R. (1995) *Chem. Res. Toxicol. 8*, 574−579.
9. Reen, R. K., Ramakanth, S., Wiebel, F. J., Jain, M. P., and Singh, J. (1991) *Anal. Biochem. 194*, 243−249.
10. Kedzie, K. M., Philpot, R. M., and Halpert, J. R. (1991) *Arch. Biochem. Biophys. 291*, 176−186.
11. Ryan, R., Grimm, S. W., Kedzie, K. M., Halpert, J. R., and Philpot, R. M. (1993) *Arch. Biochem. Biophys. 304*, 454−463.
12. Graves, P. E., Elhag, G. A., Ciaccio, P. J., Bourque, D. P., and Halpert, J. R. (1990) *Arch. Biochem. Biophys. 281*, 106−115.
13. Kedzie, K. M., Grimm, S. W., Chen, F., and Halpert, J. R. (1993) *Biochim. Biophys. Acta 1164*, 124−132.
14. Hasler, J. A., Harlow, G. R., Szklarz, G. D., John, G. H., Kedzie, K. M., Burnett, V. L., He, Y. A., Kaminsky, L. S., and Halpert, J. R. (1994) *Mol. Pharmacol. 46*, 338−345.
15. He, Y. A., Luo, Z., Klekotka, P. A., Burnett, V. L., and Halpert, J. R. (1994) *Biochemistry 33*, 4419−4424.
16. Szklarz, G. D., He, Y. A., and Halpert, J. R. (1995) *Biochemistry 34*, 14312−14322.
17. Harlow, G. R., and Halpert, J. R. (1996) *Arch. Biochem. Biophys. 326*, 85−91.
18. Szklarz, G. D., He, Y. Q., Kedzie, K. M., Halpert, J. R., and Burnett, V. L. (1996) *Arch. Biochem. Biophys. 327*, 308−318.
19. von Wachenfeld, C., and Johnson, E. F. (1995) in *Cytochrome P450: Structure, Mechanism, and Biochemistry* (Ortiz de Montellano, P. R., Ed.) pp 183−223, Plenum Press, New York.
20. Loida, P. J., and Sligar, S. G. (1993) *Biochemistry 32*, 11530−11538.
21. Mueller, E. J., Loida, P. J., and Sligar, S. G. (1995) in *Cytochrome P450: Structure, Mechanism, and Biochemistry* (Ortiz de Montellano, P. R., Ed.) pp 83−124, Plenum Press, New York.
22. Gelb, M. H., Heimbrook, D. C., Malkonen, P., and Sligar, S. G. (1982) *Biochemistry 21*, 370−377.
23. Gould, P. G., Gelb, M. H., and Sligar, S. G. (1981) *J. Biol. Chem. 256*, 6686−6691.
24. Fang, X., Kobayashi, Y., and Halpert, J. R. (1997) *FEBS Lett. 416*, 77−80.
25. Okuno, H., Nakanishi, S., Kitao, Y., Takasu, M., Murase, T., Shiozaki, Y., and Sameshima, Y. (1989) *Jpn. J. Pharmacol. 50*, 1−9.
26. Fry, J. R., Garle, M. J., and Lal, K. (1992) *Xenobiotica 22*, 211−215.
27. Nishibe, Y., and Hirata, H. (1993) *Xenobiotica 23*, 681−692.
28. Imai, Y. (1979) *J. Biochem. 86*, 1697−1707.
29. Greenlee, W. F., and Poland, A. (1978) *J. Pharmacol. Exp. Ther. 205*, 596−605.
30. Deluca, J. G., Dysart, G. R., Ransnick, D., and Bradley, M. O. (1988) *Biochem. Pharmacol. 37*, 1731−1739.
31. Matsubara, T., Otsubo, S., Yoshihara, E., and Touchi, A. (1983) *Jpn. J. Pharmacol. 33*, 41−56.
32. Harlow, G. R., and Halpert, J. R. (1997) *J. Biol. Chem. 272*, 5396−5402.
33. John, G. H., Hasler, J. A., He, Y. A., and Halpert, J. R. (1994) *Arch. Biochem. Biophys. 314*, 367−375.
34. Ueno, K. (1985) *Acta Crystallogr. C41*, 1786−1789.
35. Paulsen, M. D., and Ornstein, R. L. (1991) *Proteins 11*, 184−204.
36. Paulsen, M. D., and Ornstein, R. L. (1992) *J. Comput.-Aided Mol. Des. 6*, 449−460.
37. He, K., He, Y. A., Szklarz, G. D., Halpert, J. R., and Correia, M. A. (1996) *J. Biol. Chem. 271*, 25864−25872.
38. Szklarz, G. D., and Halpert, J. R. (1997) *J. Comput.-Aided Mol. Des. 11*, 265−272.
39. Harada, N., Miwa, G. T., Walsh, J. S., and Lu, A. Y. H. (1984) *J. Biol. Chem. 259*, 3005−3010.

BI9731450